Comput Visual Sci 3: 185–195 (2001)

Computing and
Visualization in Science
© Springer-Verlag 2001

Regular article

Slow and fast diffusion effects in image processing

Jozef Kačur[1], **Karol Mikula**[2]

[1] Comenius University, Faculty of Mathematics and Physics, Dept. of Numerical Analysis and Optimization, Mlynska Dolina, 842 15 Bratislava, Slovakia (e-mail: kacur@fmph.uniba.sk)
[2] Slovak Technical University, Dept. of Mathematics, Radlinskeho 11, 813 68 Bratislava, Slovakia (e-mail: mikula@vox.svf.stuba.sk)

Received: 6 May 1998 / Accepted: 27 July 2000

Communicated by: G. Wittum

Abstract. A mathematical model for a nonlinear image multiscale analysis is studied. Processing of an image is based on a solution of the strongly nonlinear parabolic partial differential equation, which can degenerate depending on values of the greylevel intensity function. The governing PDE is a generalization of the regularized (in the sense of Catté, Lions, Morel and Coll) Perona-Malik anisotropic diffusion equation. We present numerical techniques for solving the suggested initial-boundary value problem and also existence and convergence results. Numerical experiments are discussed.

1 Introduction

In the present paper we study the following nonlinear diffusion problems. Let $u(t,x)$ be a function (representing the greylevel intensity function in image multiscale analysis – see [2, 3, 21, 30]) which satisfies one of the PDEs:

$$\partial_t b(x,u) - \nabla(g(|\nabla G_\sigma * \beta(x,u)|)\nabla\beta(x,u)) = f(u_0 - u) \tag{1.1a}$$

or

$$\partial_t b(x,u) - \nabla(g(|\nabla G_\sigma * b(x,u)|)\nabla\beta(x,u)) = f(u_0 - u)\,, \tag{1.1b}$$

for $t \in I \equiv [0,T]$, $x \in \Omega \subset \mathbb{R}^N$, where Ω is a bounded domain with Lipschitz continuous boundary ($N = 2$ or 3 in practice of the image analysis). The equations are coupled with boundary and initial conditions of the form

$$\partial_\nu \beta(x,u) = 0 \quad \text{on } I \times \partial\Omega\,, \tag{1.2}$$

$$b(x,u(0,x)) = b(x,u_0(x))\,. \tag{1.3}$$

For the data in (1.1)–(1.3) we assume that

(H1) g is a Lipschitz continuous function, $g(0) = 1$ and $0 < g(s) \to 0$ for $s \to \infty$,

(H2) $G_\sigma \in C^\infty(\mathbb{R}^N)$ is a compactly supported smoothing kernel ($\int_{\mathbb{R}^N} G_\sigma(x)dx = 1$, $G_\sigma(x) \to \delta_x$ – Dirac measure at point x, for $\sigma \to 0$),

(H3) f is a Lipschitz continuous, nondecreasing function, $f(0) = 0$,

(H4) $u_0 \in L_2(\Omega)$ (represents the processed image).

By the term $\nabla G_\sigma * v$ we mean $\int_{\mathbb{R}^N} \nabla G_\sigma(x-\xi)\tilde{v}(\xi)d\xi$, where $\tilde{v}$ is an extension of v, for which we assume

$$\|\tilde{v}\|_{W_2^1(\mathbb{R}^N)} \le C\|v\|_{W_2^1(\Omega)}\,. \tag{1.4}$$

We consider following four cases for the shape of the functions b and β which indicate the structure of the governing equations:

(I) $b(x,s)$ is continuous, strictly increasing in s, $b(x,0) = 0$ and $\beta(x,s) \equiv s$,

(II) $b(x,s)$ is nondecreasing Lipschitz continuous in s, $b(x,0) = 0$ and $\beta(x,s) \equiv s$,

(III) $\beta(x,s)$ is continuous, strictly increasing in s, $\beta(x,0) = 0$, and $b(x,s) \equiv s$,

(IV) $\beta(x,s)$ is nondecreasing Lipschitz continuous in s, $\beta(x,0) = 0$ and $b(x,s) \equiv s$.

The initial-boundary value problems (1.1)–(1.3) in form a or b, in all cases **I-IV** are generalizations of the regularized (in the sense of Catté, Lions, Morel and Coll) Perona-Malik nonlinear diffusion equation. The Perona-Malik equation as well as its regularization are also called *anisotropic diffusion* in the computer vision community and they are widely used for image selective smoothing and edge detection in the image processing applications. The previous papers ([7, 16, 29]) have been dealing with the case when both $\beta(x,s) \equiv s$, $b(x,s) \equiv s$. In such case, the image analysis depends strongly on ∇u ([29]) or $\nabla G_\sigma * u$ ([7]) which are considered as edge indicators. Such special PDEs selectively diffuse the image in the regions, where the signal is of a constant mean in spite of those regions where the signal changes its tendency. This requirement is treated by the properties of the function g (see (H1)) originally designed in [29]. Catté, Lions, Morel and Coll introduced the regularizing convolution term (they put ∇u_σ, $u_\sigma \equiv G_\sigma * u$ instead of ∇u inside the function g) in order to preveal mathematical troubles of the original Perona-Malik formulation for the functions g used in practice ($g(s) = 1/(1+s^2)$, $g(s) = e^{-s}$). It can be seen ([2]) that, if the product $g(s)s$ is decreasing function for some s then the Perona-Malik model can behave locally like the backward heat equation, which is well-known as ill-posed problem. The slight modification using the convolution allowed to prove existence and uniqueness of the solution for the regularized problem and, from practical point of view, it keeps all advantages of the original Perona-Malik equation (see [7]). Moreover, using the convolution Catté, Lions, Morel and Coll has made explicit a *presmoothing* implicitely included in discrete numerical schemes solving the anisotropic diffusion equation in the original Perona-Malik form.

In the present paper, we add new nonlinearities represented by the functions b and β which make the image multiscale analysis locally dependent on values of the intensity function u and on the position in the image x. Such generalization is useful in any situation when properties of the image and/or requirements to the image processing operation are known a-priori and can be expressed in dependence on x and/or u. E.g., if a different speed of diffusion process is desirable in different parts of the image or for different ranges of the intensity function, the new models can be clearly used. In the points, where the derivative β'_s is small (b'_s is large) the diffusion process is slowed down while where β'_s is large (b'_s is small) the diffusion process is fasted up. We have included degenerate cases from the point of view of the theory of parabolic PDEs when either β'_s or b'_s is equal 0 or ∞. In the case **I** we admit degeneracies $b'_s = 0$ and/or ∞ in some points of intensity range, in case **II** the degeneracy $b'_s = 0$ is possible for interval ranges of intensity function and the similar is assumed considering the function $\beta(s)$ in the cases **III** and **IV**. The degenerate cases can be interpreted as total stopping of diffusion respectively as diffusion with the infinite speed in some image regions.

Applying the anisotropic diffusion (with a given smooth function g) together with the explicit/implicit presmoothing to any image u_0 improves some set of edges. On the other hand, it destroys the details which are under the edge threshold (given by g) or undistinguished from the noise in some scale. If such details are contained in the certain ranges of greylevels, then they can be conserved by the special choice of the function β or b. As a demonstration we present Fig. 3 from Sect. 4. In that image, the colors of Flora's face are demaged only. We present the reconstruction of the original (left image) by anisotropic diffusion (image in the middle) and by anisotropic diffusion accompanied with the *slow diffusion effect* – the model (1.1)–(1.3) in the case **IV** (image in the right). Using the proper choice of β, which is constant for the lower (darker) greylevels and linear for the upper range of u, the face is selectively smoothed and details around are conserved.

Due to the strong nonlinearity and possible degeneracy in (1.1), the proof of existence of a solution and its numerical approximation needs nonstandard techniques, especially, if we want to prove its convergence to the solution. We use a special approximation (see numerical schemes 2.1, 2.2) which in a constructive way look for the solution and can be implemented for the computational purposes. It is based on the special time discretization developed and applied in [6, 9–13, 15, 22–24] for solving the Stefan-like problems, flow in porous media (including saturated-unsaturated zones), mean curvature flow of convex curves in a plane, affine invariant multiscale shape analysis and further related free boundary problems. In the present paper, we use those ideas together with the techniques developed in [7] and [16] to obtain existence of a weak solution of (1.1)–(1.3) and to prove convergence of the suggested approximations.

In Sect. 2, we present approximation schemes for solving numerically the initial-boundary value problems (1.1)–(1.3). Section 3 is devoted to analysis of the existence of a weak solution and convergence of the approximations. In Sect. 4, we discuss numerical experiments with real and artificial images in order to show new features of the models.

2 Approximation schemes

In this Section we introduce the numerical technique for solving the problems (1.1)–(1.3) in all partial cases.

*2.1 Approximation scheme (for the cases **I** and **II**):*

Let $n \in \mathbb{N}$ and $\tau = \frac{T}{n}$ be the time-scale step. On each discrete time-scale level $t_i = i\tau$, $i = 0, \ldots, n$ we look for the solution θ_i ($\theta_i \approx u_i$, $u_i \approx u(t_i, x)$) of the regular elliptic problem

$$\begin{aligned}&\lambda_i(\theta_i - u_{i-1}) - \tau\nabla(g(|\nabla G_\sigma * u_{i-1}|)\nabla\theta_i)\\ &= \tau f(u_0 - u_{i-1}) \quad \text{in } \Omega\,,\\ &\partial_\nu\theta_i = 0 \quad \text{on } I \times \partial\Omega\,,\end{aligned} \tag{2.1.1a}$$

where $\lambda_i \in L_\infty(\Omega)$ is the *relaxation function* connected with the θ_i by the *convergence condition*

$$\begin{aligned}&\frac{1}{2}\tau^d \le \lambda_i\\ &\le \min\left\{\frac{b_n(x, u_{i-1} + \alpha(\theta_i - u_{i-1})) - b_n(x, u_{i-1})}{\theta_i - u_{i-1}}, K\right\}\,,\end{aligned} \tag{2.1.2}$$

where $\alpha \in (0, 1)$ (α close to 1), $0 < K$ (large), $d \in (0, 1)$ are parameters of the method and

$$b_n(x, s) := b(x, s) + \tau^d s\,. \tag{2.1.3}$$

The function u_i is obtained by the *algebraic correction*

$$b_n(x, u_i) := b_n(x, u_{i-1}) + \lambda_i(\theta_i - u_{i-1})\,. \tag{2.1.4}$$

In the case b we solve in every discrete time-scale step the equation

$$\begin{aligned}&\lambda_i(\theta_i - u_{i-1}) - \tau\nabla(g(|\nabla G_\sigma * b_n(x, u_{i-1})|)\nabla\theta_i)\\ &= \tau f(u_0 - u_{i-1})\,.\end{aligned} \tag{2.1.1b}$$

*2.2 Approximation scheme (for the cases **III** and **IV**):*

Let $n \in \mathbb{N}$ and $\tau = \frac{T}{n}$ be the time-scale step. On each discrete time-scale level $t_i = i\tau$, $i = 1, \ldots, n$ we look for the solution θ_i ($\theta_i \approx \beta(x, u_i)$, $u_i \approx u(t_i, x)$) of the regular elliptic problem

$$\mu_i(\theta_i - \beta(x, u_{i-1})) - \tau\nabla(g(|\nabla G_\sigma * u_{i-1}|)\nabla\theta_i) = \tau f(u_0 - u_{i-1}) \quad \text{in } \Omega$$

$$\partial_\nu \theta_i = 0 \quad \text{on } I \times \partial\Omega\,, \tag{2.2.1b}$$

where $\mu_i \in L_\infty(\Omega)$ is the relaxation function, connected with θ_i by the convergence condition

$$\frac{1}{2}\tau^d \le \mu_i \le \min\left\{\frac{\beta_n^{-1}(x, \beta_n(x, u_{i-1}) + \alpha(\theta_i - \beta(x, u_{i-1}))) - u_{i-1}}{\theta_i - \beta(x, u_{i-1})}, K\right\}, \tag{2.2.2}$$

where $\alpha \in (0, 1)$ (α close to 1), $0 < K$ (large), $d \in (0, 1)$ are parameters of the method and

$$\beta_n(x, s) := \beta(x, s) + \tau^d s\,. \tag{2.2.3}$$

The function u_i is obtained by the algebraic correction

$$u_i := u_{i-1} + \mu_i(\theta_i - \beta(x, u_{i-1}))\,. \tag{2.2.4}$$

In the case a we solve in every discrete time-scale step the equation

$$\mu_i(\theta_i - \beta(x, u_{i-1})) - \tau\nabla(g(|\nabla G_\sigma * \beta(x, u_{i-1})|)\nabla\theta_i) = \tau f(u_0 - u_{i-1})\,. \tag{2.2.1a}$$

Neither scheme 2.1, nor 2.2, is explicit with respect to λ_i, θ_i, μ_i, θ_i, respectively. However, they are powerfull theoretical and practical techniques for solving the nonlinear degenerate parabolic equations. Due to the properties of λ_i, μ_i and from the structure of the linear elliptic equations (2.1.1),(2.2.1), the existence of the solution θ_i is guarranteed by the theory of monotone operator's equations (see e.g. [8]). By means of the relaxation functions we control the nonlinearities (degeneracies) in the equations. They correspond to $b'_s(x, \xi)$, $1/\beta'_s(x, \xi)$, respectively, in some $\xi \in (u_{i-1}, u_i)$. The range, given by the convergence conditions is rather large. The simplest possibility is to choose e.g. $\lambda_i = \frac{1}{2}\tau^d = \mu_i$, and the couples (2.1.1)–(2.1.2),(2.2.1)–(2.2.2), respectively, are fulfilled. However, from the background of the method, a reasonable approximation has to force the relaxation functions to be close to the difference quotients in the right hand sides of the convergence conditions. For this purpose, we use iterations (described in Remarks 2.6, 2.7) similar to ones from [10, 12, 13, 24]. We can expect that some other semiimplicit ([31]), implicit ([27]) or explicit (widely used in image analysis) computational techniques can be successfull for some special cases of (1.1)–(1.3). In the numerical implementation we can put also $\alpha = 1$ which simplifies the formulas. Then, in the optimal case (of the choice of λ_i, μ_i) we actually have to solve the corresponding nonlinear elliptic problem; e.g., in the case $(\mathbf{IV})_b$ it is

$$\beta_n^{-1}(x, \theta_i) - \tau\nabla(g(|\nabla G_\sigma * u_{i-1}|)\nabla\theta_i) = u_{i-1} + \tau f(u_0 - u_{i-1})\,,$$

which can be treated in an iterative way (see (2.7.1)–(2.7.4)).

Remark 2.3. In fact, both degeneracies (under the time derivative and in the divergence term) can be included using simultaneously $b(x, s)$ and $\beta(x, s)$ provided they are strictly increasing in s. However, we can invert $b(x, s)$ or $\beta(x, s)$ and transform the problem into the form **I** or **III**. For completness we present also the scheme for the general situation. It uses two relaxation functions balanced in the optimal way by two conditions. Convergence can be obtained by the similar arguments as in Sect. 3 (for technical details see also [13]).

On each discrete time-scale level $t_i = i\tau$, $i = 0, \ldots, n$ we look for the solution θ_i ($\theta_i \approx \beta(x, u_i)$, $u_i \approx u(t_i, x)$) of the regular elliptic problem

$$\lambda_i(\theta_i - \beta(x, u_{i-1})) - \tau\nabla(g(|\nabla G_\sigma * u_{i-1}|)\nabla\theta_i) = \tau f(u_0 - u_{i-1})$$

$$\partial_\nu \theta_i = 0 \quad \text{on } I \times \partial\Omega\,,$$

where $\lambda_i \in L_\infty(\Omega)$ satisfies

$$\frac{1}{2}\tau^d \le \lambda_i \le \min\left\{\frac{b_n(x, u_{i-1} + \mu_i(\theta_i - \beta(x, u_{i-1}))) - b_n(x, u_{i-1})}{\theta_i - \beta(x, u_{i-1})}, K\right\},$$

with $\mu_i \in L_\infty(\Omega)$

$$0 \le \mu_i \le \min\left\{\frac{\beta_n^{-1}(x, \beta_n(x, u_{i-1}) + \alpha(\theta_i - \beta(x, u_{i-1}))) - u_{i-1}}{\theta_i - \beta(x, u_{i-1})}, K\right\},$$

where $\alpha \in (0, 1)$ (α close to 1), $0 < K$ (large), $d \in (0, 1)$ are parameters of the method. The function u_i is determined from

$$b_n(x, u_i) := b_n(x, u_{i-1}) + \lambda_i(\theta_i - \beta(x, u_{i-1}))\,.$$

If $\beta(x, s) \equiv s$, we can take $\mu_i = \alpha$ to obtain Approximation scheme 2.1. When $b(x, s) \equiv s$ we can take $\lambda_i = \mu_i$ to obtain Aproximation scheme 2.2.

In what follows, we understand the solutions of (2.1.1), and (2.2.1), respectively, in variational sense. It means, that we look for $\theta_i \in V$, satisfying the following identities

$$(\lambda_i(\theta_i - u_{i-1}), v) + \tau(g(|\nabla G_\sigma * u_{i-1}|)\nabla\theta_i, \nabla v) = \tau(f(u_0 - u_{i-1}), v) \tag{2.4a}$$

$$(\lambda_i(\theta_i - u_{i-1}), v) + \tau(g(|\nabla G_\sigma * b_n(x, u_{i-1})|)\nabla\theta_i, \nabla v) = \tau(f(u_0 - u_{i-1}), v) \tag{2.4b}$$

$$(\mu_i(\theta_i - \beta(x, u_{i-1})), v) + \tau(g(|\nabla G_\sigma * \beta(x, u_{i-1})|)\nabla\theta_i, \nabla v) = \tau(f(u_0 - u_{i-1}), v)\,, \tag{2.5a}$$

$$(\mu_i(\theta_i - \beta(x, u_{i-1})), v) + \tau(g(|\nabla G_\sigma * u_{i-1}|)\nabla\theta_i, \nabla v) = \tau(f(u_0 - u_{i-1}), v)\,, \tag{2.5b}$$

for every $v \in V$,where $V \equiv W_2^1(\Omega)$ is Sobolev space.

Now we introduce iteration processes suitable for determination of relaxation functions, which are close to the difference quotients in the right hand sides of the convergence conditions.

Remark 2.6. The couple θ_i, λ_i simultaneously satisfying (2.1.1),(2.1.2) is determined iteratively by the following scheme

$$(\lambda_{i,k-1}(\theta_{i,k}-u_{i-1}), v) + \tau(g(|\nabla G_\sigma * u_{i-1}|)\nabla\theta_{i,k}, \nabla v) = \tau(f(u_0-u_{i-1}), v) \tag{2.6.1a}$$

$$\overline{\lambda}_{i,k} = \min\left\{\frac{b_n(u_{i-1}+\alpha(\theta_{i,k}-u_{i-1}))-b_n(u_{i-1})}{\theta_{i,k}-u_{i-1}}, K\right\}, \tag{2.6.2}$$

$$\lambda_{i,k} := \overline{\lambda}_{i,k}, \quad \text{for } 1 \le k \le k_0,$$
$$\lambda_{i,k} := \min\{\overline{\lambda}_{i,k}, \lambda_{i,k-1}\}, \quad \text{for } k = k_0+1\ldots, \tag{2.6.3}$$

starting this process with

$$\lambda_{i,0} = \min\{\alpha(b_n)'_s(x, u_{i-1}), K\}. \tag{2.6.4}$$

If $\theta_{i,k} = u_{i-1}$ then we put $\overline{\lambda}_{i,k} = \lambda_{i,0}$.

Remark 2.7. The couple θ_i, μ_i simultaneously satisfying (2.2.1)–(2.2.2) is determined iteratively by the following scheme

$$(\mu_{i,k-1}(\theta_{i,k}-\beta(x, u_{i-1})), v) + \tau(g(|\nabla G_\sigma * u_{i-1}|)\nabla\theta_{i,k}, \nabla v) = (f(u_0-u_{i-1}), v) \tag{2.7.1b}$$

$$\overline{\mu}_{i,k} = \min\left\{\frac{\beta_n^{-1}(x, \beta_n(x, u_{i-1})+\alpha(\theta_{i,k}-\beta(x, u_{i-1})))-u_{i-1}}{\theta_{i,k}-\beta(x, u_{i-1})}, K\right\} \tag{2.7.2}$$

$$\mu_{i,k} := \overline{\mu}_{i,k}, \quad \text{for } 1 \le k \le k_0,$$
$$\mu_{i,k} := \min\{\overline{\mu}_{i,k}, \mu_{i,k-1}\}, \quad \text{for } k = k_0+1, \ldots. \tag{2.7.3}$$

The iterations are starting with

$$\mu_{i,0} = \min\{\alpha/\beta'_s(x, u_{i-1}), K\}. \tag{2.7.4}$$

Note that, if $\theta_{i,k} = \beta(x, u_{i-1})$ then we put $\overline{\mu}_{i,k} = \mu_{i,0}$.

By the previous constructions with $k_0 \ge 1$, the sequences $\{\mu_{i,k}\}$, $\{\lambda_{i,k}\}$ are forced to be monotone and hence convergent. The corresponding sequences of unknown functions $\theta_{i,k}$ in the elliptic equations converge in some functional spaces, too. The limit functions fulfill (2.1.1)–(2.1.2), (2.2.1)–(2.2.2), respectively. The proof of that facts can be obtained in the similar lines as in [12–14, 24]. In practical implementations k_0 can be choosen in accordance with the shape of β, and b (e.g. sufficiently large, if the numerical convergence of $\overline{\mu}_{i,k}$, $\overline{\lambda}_{i,k}$, respectively, is observed).

We denote $Q_T = I \times \Omega$, the scalar product in $L_2(\Omega)$ by $(\cdot,\cdot)$ and duality between V and V^* by $<\cdot,\cdot>$. We use symbols $|\cdot|_2, \|\cdot\|, \|\cdot\|_*, |\cdot|_\infty, |\cdot|_p$ for norms in $L_2(\Omega)$, V, V^*, $L_\infty(\Omega)$ and $L_p(\Omega)$ (see e.g [20]). By $\to$, $\rightharpoonup$ we mean the strong and weak convergence. By $C, C_1, \ldots$ we denote general (large) constants.

By means of u_i, θ_i, determined by Approximation schemes 2.1, 2.2, in each discrete time-scale step, we construct Rothe's functions

$$u^{(n)}(t) = u_{i-1} + \frac{t-t_{i-1}}{\tau}(u_i - u_{i-1}),$$
$$\text{for } t_{i-1} \le t \le t_i,\ i = 1, \ldots, n$$

$$\overline{u}^{(n)}(t) = u_i, \quad \text{for } t_{i-1} < t \le t_i,\ i = 1, \ldots, n, \quad \overline{u}^{(n)}(0) = u_0.$$

$$\theta^{(n)}(t) = \theta_{i-1} + \frac{t-t_{i-1}}{\tau}(\theta_i - \theta_{i-1}),$$
$$\text{for } t_{i-1} \le t \le t_i,\ i = 1, \ldots, n$$

$$\overline{\theta}^{(n)}(t) = \theta_i, \quad \text{for } t_{i-1} < t \le t_i,\ i = 1, \ldots, n, \quad \overline{\theta}^{(n)}(0) = \theta_0. \tag{2.8}$$

They are considered as the approximations of a weak solution of (1.1)–(1.3) defined by

Definition 1. *A measurable function $u : Q_T \to \mathbb{R}$ is a weak solution of* (1.1a)–(1.3) *iff*

(i) $\partial_t b(x,u) \in L_2(I, V^*)$, $\beta(x,u) \in L_2(I, V)$
(ii) $\int_I <\partial_t b(x,u), v> = -\int_{Q_T}(b(x,u)-b(x,u_0))\partial_t v$, $\forall v \in V \cap L_\infty(Q_T)$ *with* $\partial_t v \in L_\infty(Q_T)$, $v(T,x) = 0$,
(iii)$_a$ $\int_I <\partial_t b(x,u), v> + \int_I(g(|\nabla G_\sigma * \beta(x,u)|)\nabla\beta(x,u), \nabla v) = \int_I(f(u_0-u), v)\forall v \in L_2(I,V)$.

In the similar way we define a weak solution of (1.1b)–(1.3). *It is clear how to understand this Definition in the partial cases **I-IV**.*

The next Section concerns the convergence of Rothe's functions (2.8) to corresponding weak solutions.

3 Convergence results

Case I.
In this Section, we assume some further technical assumptions:

(H5) $|f(s)| \le C(1+|s|)$,

(H6) $C_1 s^2 - C_2 \le b(x,s)s \le C_3 + C_4 s^2$,

(H7) $|b'_s(x+y,s) - b'_s(x,s)| \le \omega(|y|)(1+b'_s(x,s))$,
where $\omega : \mathbb{R}_+ \to \mathbb{R}_+$ is continuous, $\omega(0) = 0$.

Let us denote

$$\Phi_n(x,s) := \int_0^s b_n(x,z)dz$$

and

$$B_n(x,s) := b_n(x,s)s - \int_0^s b_n(x,z)dz = b_n(x,s)s - \Phi_n(x,s).$$

Similarly we define $\Phi(x,s)$, $B(x,s)$ replacing $b_n(x,s)$ by $b(x,s)$.

The Lax-Milgram theorem guarrantees the existence of a solution $\theta_i \in V$ in (2.4a), (2.4b), respectively, for every $i = 1, \ldots, n$.

Lemma 1. *The a priori estimates*

$$\max_{1\le i\le n}\int_\Omega B_n(x,u_i)\le C,\quad \sum_{i=1}^n \|\theta_i\|^2\tau\le C,$$
$$\sum_{i=1}^n\int_\Omega \frac{1}{\lambda_i}(b_n(x,u_i)-b_n(x,u_{i-1}))^2\le C$$

hold uniformly with respect to n.

Proof. Let us test (2.4a), (2.4b), respectively by θ_i and sum it up for $i=1,\dots,j$. Applying (2.1.4), Young's inequality and the assumption (H5) we obtain

$$\begin{aligned}&\sum_{i=1}^j(b_n(x,u_i)-b_n(x,u_{i-1}),\frac{1}{\lambda_i}(b_n(x,u_i)-b_n(x,u_{i-1})))\\&+\sum_{i=1}^j(b_n(x,u_i)-b_n(x,u_{i-1}),u_i)\\&-\sum_{i=1}^j(b_n(x,u_i)-b_n(x,u_{i-1}),u_i-u_{i-1})\\&+\sum_{i=1}^j\gamma_i(u_{i-1})|\nabla\theta_i|_2^2\tau\le C_1\sum_{i=1}^j(|u_{i-1}|_2^2+|\theta_i|_2^2)\tau+C_2\,,\end{aligned}\tag{3.1}$$

where $\gamma_i(u_{i-1})=g(|\nabla G_\sigma*u_{i-1}|)\ge 0$ ($\gamma_i(u_{i-1})=g(|\nabla G_\sigma* b_n(x,u_{i-1})|)\ge 0$ in case b)). From (2.1.2) and (2.1.4) we have

$$\begin{aligned}&|b_n(x,u_i)-b_n(x,u_{i-1})|=|\lambda_i(\theta_i-u_{i-1})|\\&\le|b_n(x,u_{i-1}+\alpha(\theta_i-u_{i-1}))-b_n(x,u_{i-1})|\end{aligned}$$

and thus from the strict monotonicity of $b_n(x,s)$ in s we obtain

$$\begin{aligned}|u_i-u_{i-1}|&\le\alpha|\theta_i-u_{i-1}|\\&=\alpha\left|\frac{1}{\lambda_i}(b_n(x,u_i)-b_n(x,u_{i-1}))\right|\,,\end{aligned}$$

which implies the relation between the first and third term in (3.1)

$$\begin{aligned}&\left|\sum_{i=1}^j(b_n(x,u_i)-b_n(x,u_{i-1}),u_i-u_{i-1})\right|\\&\le\alpha\sum_{i=1}^j\int_\Omega\frac{1}{\lambda_i}(b_n(x,u_i)-b_n(x,u_{i-1}))^2\,.\end{aligned}\tag{3.2}$$

From the inequality

$$(u_i-u_{i-1})b_n(x,u_{i-1})\le\Phi_n(x,u_i)-\Phi_n(x,u_{i-1})\,,$$

we have

$$\begin{aligned}&\sum_{i=1}^j(b_n(x,u_i)-b_n(x,u_{i-1}),u_i)\ge(b_n(x,u_j),u_j)\\&\qquad-(b_n(x,u_0),u_0)-\sum_{i=1}^j(u_i-u_{i-1},b_n(x,u_{i-1}))\\&\ge(b_n(x,u_j),u_j)-(b_n(x,u_0),u_0)\\&\qquad-\sum_{i=1}^j\int_\Omega(\Phi_n(x,u_j)-\Phi_n(x,u_{i-1}))\\&=\int_\Omega B_n(x,u_j)-\int_\Omega B_n(x,u_0)\,.\end{aligned}\tag{3.3}$$

Due to (2.1.4) we obtain

$$|\theta_i|_2^2\le 2\int_\Omega\frac{1}{\lambda_i^2}(b_n(x,u_i)-b_n(x,u_{i-1}))^2+2|u_{i-1}|_2^2\tag{3.4}$$

and by the asymptotical properties of $b(x,s)$ (see (H6)) we have the relation $B_n(x,s)\ge C_1s^2-C_2$ which implies

$$|u_i|_2^2\le C_1\int_\Omega B_n(x,u_i)+C_2\,.\tag{3.5}$$

Applying (3.2)–(3.5) in (3.1) we obtain

$$\begin{aligned}&\int_\Omega B_n(x,u_j)+(1-\alpha)\sum_{i=1}^j\int_\Omega\frac{1}{\lambda_i}(b_n(x,u_i)-b_n(x,u_{i-1}))^2\\&\qquad+\sum_{i=1}^j\gamma_i(u_{i-1})|\nabla\theta_i|_2^2\tau\\&\le C_1+C_2\tau\sum_{i=1}^j\int_\Omega B_n(x,u_i)\\&\qquad+C_3\tau\sum_{i=1}^j\int_\Omega\frac{1}{\lambda_i^2}(b_n(x,u_i)-b_n(x,u_{i-1}))^2\,.\end{aligned}\tag{3.6}$$

Then for $\tau\le\tau_0$ due to the properties of λ_i and by Gronwall's argument we obtain

$$\begin{aligned}&\max_{1\le i\le n}\int_\Omega B_n(x,u_i)\le C\,,\\&\sum_{i=1}^n\int_\Omega\frac{1}{\lambda_i}(b_n(x,u_i)-b_n(x,u_{i-1}))^2\le C\,.\end{aligned}\tag{3.7}$$

Using (H2), (3.7), Young's inequality and asymptotical properties of b we estimate

$$\begin{aligned}&\left|\frac{\partial}{\partial x_i}G_\sigma*u_{i-1}\right|\le\int_{\mathbb{R}^N}B_n^*\left(x,\frac{\partial}{\partial x_i}G_\sigma\right)+\int_{\mathbb{R}^N}B_n(x,u_{i-1})\\&\le C_1+C_2\int_\Omega B_n(x,u_{i-1})\le C\,,\end{aligned}\tag{3.8}$$

where $B_n^*(x,s)$ is a conjugate to the convex function $B_n(x,s) \geq 0$ (see [1, 19]). Thus

$$|\nabla G_\sigma * u_{i-1}| \leq C < \infty$$

and so

$$g(|\nabla G_\sigma * u_{i-1}|) \geq \nu > 0\,, \quad i = 1, \ldots, n\,, \tag{3.9}$$

which implies the second estimate stated in the lemma for the case a. In the case b, we use

$$\begin{aligned}&\left|\frac{\partial}{\partial x_i} G_\sigma * b_n(x, u_{i-1})\right| \\ &\leq \int_{\mathbb{R}^N} \Phi_n\left(x, \frac{\partial}{\partial x_i} G_\sigma\right) + \int_{\mathbb{R}^N} \Psi_n(b_n(x, u_{i-1})) \\ &\leq C_3 + C_4 \int_\Omega B_n(x, u_{i-1}) \leq C\,,\end{aligned}$$

where Ψ_n is the conjugate function to the potential Φ_n and we have used the equality $\Psi_n(b_n(x,u_{i-1})) = B_n(x,u_{i-1})$ which can be verified (see also [1]). So the proof is complete. □

Consequence 1.

$$\sum_{i=1}^n |\theta_i - u_{i-1}|_2^2 \leq C\tau^{-d}, \quad \sum_{i=1}^n |u_i - u_{i-1}|_2^2 \leq C\tau^{-d}\,.$$

Now, let us define the functions

$$\begin{aligned}\hat{b}_n(x, \overline{u}^{(n)}(t)) &:= b_n(x, u_{i-1}) \\ &\qquad + \frac{t - t_{i-1}}{\tau}(b_n(x, u_i) - b_n(x, u_{i-1}))\,, \\ &\qquad \text{for } t_{i-1} \leq t \leq t_i,\ i = 1, \ldots, n\,,\end{aligned}$$

$$\overline{u}_\tau^{(n)}(t) := \overline{u}^{(n)}(t - \tau)\,.$$

Lemma 2. *There exists $u \in L_2(I, V)$, with $\partial_t b(x,u) \in L_2(I, V^*)$ such that (in the sense of subsequences)*

$$\begin{aligned}&\overline{u}^{(n)} \to u \quad \textit{a.e. in } Q_T\,,\\ &\overline{u}^{(n)} \to u \quad \textit{in } L_s(Q_T), \forall s < 2\,,\\ &\overline{\theta}^{(n)} \to u \quad \textit{in } L_s(Q_T), \forall s < 2\,,\\ &\overline{\theta}^{(n)} \rightharpoonup u \quad \textit{in } L_2(I, V)\,,\\ &\partial_t \hat{b}_n(x, \overline{u}^{(n)}) \rightharpoonup \partial_t b(x,u) \quad \textit{in } L_2(I, V^*)\,.\end{aligned}$$

Proof. We use (2.1.4) in (2.4a) (in (2.4b), respectively) and sum it for $i = j+1, \ldots, j+k$. Let us consider $v = (\theta_{j+k} - \theta_j)\tau$ as a test function and sum it again for $j = 0, \ldots, n-k$. Using the a priori estimates of Lemma 1 and Consequence 1 we successively obtain the estimate

$$\sum_{j=0}^{n-k} (b_n(x, u_{j+k}) - b_n(x, u_j), \theta_{j+k} - \theta_j)\tau \leq Ck\tau\,, \tag{3.10}$$

which can be rewritten into the form

$$\begin{aligned}&\int_0^{T-z} (b_n(x, \overline{u}^{(n)}(t+z)) - b_n(x, \overline{u}^{(n)}(t)), \overline{\theta}^{(n)}(t+z) - \overline{\theta}^{(n)}(t)) \\ &\leq C(z+\tau)\,,\end{aligned} \tag{3.11}$$

where $k\tau \leq z \leq (k+1)\tau$. Using (2.1.4), (H6), (3.5) and the estimates of Lemma 1 and Consequence 1 we obtain

$$\begin{aligned}&\int_0^{T-z} (b_n(x, \overline{u}^{(n)}(t+z) - b_n(x, \overline{u}^{(n)}(t)), \overline{u}^{(n)}(t+z) - \overline{u}^{(n)}(t)) \\ &\leq C_1(z + \tau^{(1-d)/2})\,.\end{aligned} \tag{3.12}$$

Let us define

$$\rho(x,s) := \min\{b_s'(x,s), 1\}$$

and

$$W(x,s) := \int_0^s \rho(x,z)dz\,.$$

The function $W(x,s)$ is strictly monotone in s, and (3.12) implies

$$\int_0^{T-z}\int_\Omega (W(x, \overline{u}^{(n)}(t+z)) - W(x, \overline{u}^{(n)}(t)))^2 \leq C_2(z + \tau^{(1-d)/2})\,, \tag{3.13}$$

for all $n \geq n_0$, $0 < z \leq z_0$. The second estimate of Lemma 1 gives us

$$\int_{Q_T} (\overline{\theta}^{(n)}(t, x+y) - \overline{\theta}^{(n)}(t,x))^2 \leq \omega(|y|)\,, \tag{3.14}$$

where $|y| < y_0$ (see e.g. [26]). Then (2.1.4) and Consequence 1 imply

$$\int_{Q_T} (\overline{u}^{(n)}(t, x+y) - \overline{u}^{(n)}(t,x))^2 \leq C_3(\omega(|y|) + \tau^{(1-d)/2})\,. \tag{3.15}$$

Then from the construction of $W(x,s)$ and from (H6), (H7) we obtain

$$\begin{aligned}&\int_{Q_T} (W(x+y, \overline{u}^{(n)}(t, x+y)) - W(x, \overline{u}^{(n)}(t,x)))^2 \\ &\leq C_4(\omega(|y|) + \tau^{(1-d)/2})\,.\end{aligned} \tag{3.16}$$

The compactness of $\{W(x, \overline{u}^{(n)}(t,x))\}_{n=1}^\infty$ in $L_2(Q_T)$ follows from (3.13) and (3.16).

Since $W(x,s)$ is strictly increasing in s we have (in the sense of subsequences) that $\overline{u}^{(n)} \to u$ *a.e. in* Q_T and moreover $\overline{u}^{(n)} \to u$ *in* $L_s(Q_T)$, $\forall s < 2$. Because of Consequence 1 we have also $\overline{\theta}^{(n)} \to u$ *in* $L_s(Q_T), \forall s < 2$. From that and from the second estimate of Lemma 1 we obtain $\overline{\theta}^{(n)} \rightharpoonup u$ *in* $L_2(I, V)$.

By duality argument in (2.4a) (respectively (2.4b)), using (2.1.4) and a priori estimates of Lemma 1 and Consequence 1, we obtain

$$\|\partial_t \hat{b}_n(x, \overline{u}^{(n)})\|_{L_2(I,V^*)}^2 \leq C \int_I (1 + \|\overline{\theta}^{(n)}\|^2 + |\overline{u}_\tau^{(n)}|_2^2) \leq C$$

and hence $\partial_t \hat{b}_n(x, \overline{u}^{(n)}) \rightharpoonup \chi$ in $L_2(I, V^*)$ (in the sense of subsequences). Lemma 1 then implies

$$\int_{Q_T} (\hat{b}_n(x, \overline{u}^{(n)}) - b_n(x, \overline{u}^{(n)}))^2 \le C\tau^{1-d} \to 0\,, \quad \text{for } n \to \infty\,.$$

Since $b_n(x, s) \to b(x, s)$ locally uniformly in s, $\overline{u}^{(n)} \to u$ *a.e. in* Q_T and $\int_\Omega b_n^2(x, \overline{u}^{(n)}) \le C$ we have $b_n(x, \overline{u}^{(n)}) \to b(x, u)$ *in* $L_s(Q_T)$, $\forall s < 2$. Thus $\partial_t \hat{b}_n(x, \overline{u}^{(n)}) \rightharpoonup \partial_t b(x, u)$. □

Let us integrate (2.4a) respectively (2.4b) on $(0, t)$, $t \in I$. We obtain

$$\int_0^t (\partial_t \hat{b}_n(x, \overline{u}^{(n)}), v) + \int_0^t (g(|\nabla G_\sigma * \overline{u}_\tau^{(n)}|)\nabla\overline{\theta}^{(n)}, \nabla v)$$

$$= \int_0^t (f(u_0 - \overline{u}_\tau^{(n)}), v), \forall v \in V\,. \tag{3.17}$$

$$\int_0^t (\partial_t \hat{b}_n(x, \overline{u}^{(n)}), v) + \int_0^t (g(|\nabla G_\sigma * b_n(x, \overline{u}_\tau^{(n)})|)\nabla\overline{\theta}^{(n)}, \nabla v)$$

$$= \int_0^t (f(u_0 - \overline{u}_\tau^{(n)}), v), \forall v \in V\,. \tag{3.18}$$

We can take the limit for $n \to \infty$ in previous identities and using the convergence results of Lemma 2 and the facts that $g(|\nabla G_\sigma * \overline{u}_\tau^{(n)}|) \to g(|\nabla G_\sigma * u|)$, $g(|\nabla G_\sigma * b_n(x, \overline{u}_\tau^{(n)})|) \to g(|\nabla G_\sigma * b(x, u)|)$ *a.e in* Q_T (which follow from Consequence 1 and Lemma 2) we have the following

Theorem 1. *There exists variational solution u of the problems* (1.1)–(1.3) *in case **I**. Moreover* $\overline{u}^{(n)} \to u, \overline{\theta}^{(n)} \to u$ *in* $L_s(Q_T)$, $\forall s < 2$, *where* $\overline{u}^{(n)}, \overline{\theta}^{(n)}$ *are the sequences obtained by Approximation scheme 2.1.*

Using the results of [1] and [12], in both cases a and b, the stronger convergence result can be proved.

Theorem 2. *Let* $\overline{u}^{(n)}, \overline{\theta}^{(n)}$ *be the sequences obtained by Approximation scheme 2.1. Then*

$$\overline{u}^{(n)} \to u \quad \text{in } L_2(Q_T)\,, \quad \overline{\theta}^{(n)} \to u \quad \text{in } L_2(I, V)\,,$$

where u is a variational solution of the problems (1.1)–(1.3) *in case **I**.*

Proof. Let us test (3.17) (respectively (3.18)) by $v = \overline{\theta}^{(n)} - u$, where u is a variational solution. We have (due to the per partes formula – see [12], Lemma 3.25 or [1], Lemma 1.5)

$$\int_0^t (\partial_t \hat{b}_n(x, \overline{u}^{(n)}), u) \to \int_0^t < \partial_t b(x, u), u >$$

$$= \int_\Omega B(x, u(t)) - \int_\Omega B(x, u(0))\,. \tag{3.19}$$

Since $B_n(x, s) \to B(x, s)$ locally uniformly for bounded s, by Fatou's argument and using Lemma 2 and (3.3) we obtain

$$\begin{aligned}\underline{\lim} \int_0^t (\partial_t \hat{b}_n(x, \overline{u}^{(n)}), \overline{\theta}^{(n)}) &\ge \int_\Omega B_n(x, \overline{u}^{(n)}(t)) - \int_\Omega B_n(x, u(0)) \\ &\ge \int_\Omega B(x, u(t)) - \int_\Omega B(x, u(0))\,.\end{aligned}$$

Thus

$$\int_0^t (\partial_t \hat{b}_n(x, \overline{u}^{(n)}), \overline{\theta}^{(n)} - u) \ge o(1)\,, \tag{3.20}$$

where the Landau symbol $o(1)$ denotes a term $c_n \to 0$ for $n \to \infty$. From the growth properties of f and from the fact that $\overline{\theta}^{(n)} \to u$ *in* $L_s(Q_T)$ we have

$$\int_0^t (g(|\nabla G_\sigma * \overline{u}_\tau^{(n)}|)\nabla\overline{\theta}^{(n)}, \nabla(\overline{\theta}^{(n)} - u)) \le o(1)\,. \tag{3.21}$$

Since $0 < \nu \le g(|\nabla G_\sigma * \overline{u}_\tau^{(n)}|) \to g(|\nabla G_\sigma * u|)$ *a.e. in* Q_T and from $\overline{\theta}^{(n)} \rightharpoonup u \in L_2(I, V)$ we have

$$\int_0^t (g(|\nabla G_\sigma * \overline{u}_\tau^{(n)}|)\nabla u, \nabla(\overline{\theta}^{(n)} - u)) = o(1)\,. \tag{3.22}$$

From (3.20)–(3.22) we deduce

$$\int_0^t |\nabla(\overline{\theta}^{(n)} - u)|_2^2 \to 0 \quad \textit{for } n \to \infty\,,$$

so $\nabla\overline{\theta}^{(n)} \to \nabla u$ in $L_2(Q_T)$. The same result holds also for the case b. To prove $\overline{\theta}^{(n)} \to u$ in $L_2(Q_T)$ we use the following argument. Let us take

$$c_n = \frac{1}{|Q_T|}\int_{Q_T} \overline{\theta}^{(n)}$$

and construct

$$v^{(n)} := \overline{\theta}^{(n)} - c_n\,.$$

Since $\nabla v^{(n)} \to \nabla u$ in $L_2(Q_T)$ and $\int_{Q_T} v^{(n)} = 0$ we have that $v^{(n)}$ converges in $L_2(Q_T)$. Since c_n is bounded ($\int_I |\overline{\theta}^{(n)}|^2 \le C$) we can assume $c_n \to c$ (up to a subsequence) and hence $\overline{\theta}^{(n)} = v^{(n)} - c_n$ converges in $L_2(Q_T)$. Thus $\overline{\theta}^{(n)} \to u$ in $L_2(Q_T)$ since $\overline{\theta}^{(n)} \rightharpoonup u$ in $L_2(Q_T)$. Then also $\overline{u}^{(n)} \to u$ in $L_2(Q_T)$ and the proof is complete. □

In the analysis of the next three cases we will be more brief, because the ideas are similar to the ones used in the previous part of this Section. We will concentrate only to the main differences.

Case II. In this case we consider the right hand side of the equations in the form $f \equiv f(b(x, u_0) - b(x, u))$ and correspondingly in Approximation scheme 2.1. Instead of (H7) we assume

(H8) $|b(x+y,s)-b(x,s)| \le \omega(|y|)(1+b(x,s))$, where $\omega : \mathbb{R}_+ \to \mathbb{R}_+$ is continuous, $\omega(0)=0$.

Then, in both cases a and b, we obtain the same *a priori estimates* as in Lemma 1 and Consequence 1. Similarly as in the proof of Lemma 2 we obtain the inequality (3.10), from which and Lipschitz continuity of b we have

$$\int_0^{T-z}\int_\Omega (b_n(x,\overline{u}^{(n)}(t+z)-b_n(x,\overline{u}^{(n)}(t)))^2 \le C_1(z+\tau^{(1-d)/2}) . \tag{3.23}$$

Using (H8) we also obtain

$$\int_{Q_T} (b_n(x+y,\overline{u}^{(n)}(t,x+y)-b_n(x,\overline{u}^{(n)}(t)(t,x))^2 \le C_2(\omega(|y|)+\tau^{(1-d)/2}) , \tag{3.24}$$

from which and (3.23) follow the compactness of $\{b_n(x,\overline{u}^{(n)}\}$ in $L_2(Q_T)$. The asymptotical properties of b imply that $\int_{Q_T}|\overline{u}^{(n)}|^2 \le C$ and hence $\overline{u}^{(n)} \rightharpoonup u$ in $L_2(Q_T)$. From the compactness result we have $b_n(x,\overline{u}^{(n)}) \to \xi$ in $L_2(Q_T)$. Then

$$0 \le \int_{Q_T}(b_n(x,\overline{u}^{(n)})-b_n(x,v),\overline{u}^{(n)}-v) \to \int_{Q_T}(\xi - b(x,v),u-v) \ge 0$$

for every $v \in L_2(Q_T)$ because of the monotonicity of b_n. Hence for $v = u \pm \varepsilon w$ and $\varepsilon \to 0$ we obtain $\xi = b(x,u)$. In the similar way as in the proof of Lemma 2 we obtain $\partial_t \hat{b}_n(x,\overline{u}^{(n)}) \rightharpoonup \partial_t b(x,u)$ in $L_2(I,V^*)$. Due to *a priori estimate* $\int_I \|\overline{\theta}^{(n)}\|^2 \le C$ we obtain $\overline{\theta}^{(n)} \rightharpoonup u$ in $L_2(I,V)$ since $\int_I |\overline{\theta}^{(n)} - \overline{u}_\tau^{(n)}|^2 \to 0$. The previous considerations allow us to take limit $n \to \infty$ in (3.17), (3.18), respectively, and we conclude that u is a weak solution of (1.1)–(1.3). Then we can proceed in the similar lines as in the proof of Theorem 2 to obtain

Theorem 3. *There exists variational solution u of the problems* (1.1)–(1.3) *in case* ***II***. *Let $\overline{u}^{(n)}, \overline{\theta}^{(n)}$ be the sequences obtained by Approximation scheme 2.1. Then*

$$\overline{u}^{(n)} \to u \quad in\, L_2(Q_T) , \quad \overline{\theta}^{(n)} \to u \quad in\, L_2(I,V) .$$

Cases III and IV.

We follow the ideas from [10, 13, 15] and we only sketch the results. Instead of (H6)–(H7) we assume

(H9) $C_1 s^2 - C_2 \le \beta(x,s)s \le C_3 + C_4 s^2$,

(H10) $|\beta_s'(x+y,s) - \beta_s'(x,s)| \le \omega(|y|)(1+\beta_s'(x,s))$, where $\omega : \mathbb{R}_+ \to \mathbb{R}_+$ is continuous, $\omega(0)=0$.

In case **IV**, we consider the right hand side of the equations in the form $f \equiv f(\beta(x,u_0)-\beta(x,u))$ and correspondingly in Approximation scheme 2.2.

We denote

$$\Phi_\beta := \int_0^s \beta(x,z)dz .$$

Using the similar access as in [10] and [15] and the conjugate function to potential Φ_β similarly as in the proof of Lemma 1 (to estimate the *gaussian gradient* term) we obtain

Lemma 3. *The a priori estimates*

$$\max_{1\le i\le n}\int_\Omega \Phi_\beta(x,u_i) \le C , \quad \sum_{i=1}^n \|\theta_i\|^2\tau \le C , \quad \sum_{i=1}^n |u_i - u_{i-1}|^2 \le C$$

hold uniformly with respect to n.

Then we have also

Consequence 2.

$$\sum_{i=1}^n |\theta_i - \beta(x,u_{i-1})|^2 \le C\tau^{-d} .$$

By the similar ideas as in the proof of Lemma 2, [10, 15] and [13] we obtain the compactness of $\{\overline{\theta}^{(n)}\}$ in $L_2(Q_T)$ and then

Lemma 4. *There exists $u \in L_2(Q_T)$ with $\beta(x,u) \in L_2(I,V)$ such that $\overline{u}^{(n)} \rightharpoonup u$ in $L_2(Q_T)$, $\overline{\theta}^{(n)} \rightharpoonup \beta(x,u)$ in $L_2(I,V)$, $\partial_t u^{(n)} \rightharpoonup \partial_t u$ in $L_2(I,V^*)$.*

Now we can use (see [1, 15]) the relations

$$\underline{\lim}\int_0^t < \partial_t u^{(n)}, \overline{\theta}^{(n)}) > \ge \int_\Omega \Phi_\beta(x,u(t)) - \int_\Omega \Phi_\beta(x,u_0) ,$$

$$\int_0^t < \partial_t u, \beta(x,u) > = \int_\Omega \Phi_\beta(x,u(t)) - \int_\Omega \Phi_\beta(x,u_0)$$

to prove

Theorem 4. *There exist weak solution of the problems* (1.1)–(1.3) *in cases* ***III, IV***. *Let $\overline{u}^{(n)}, \overline{\theta}^{(n)}$ be the sequences obtained by Approximation scheme 2.2. Then*

$$\overline{u}^{(n)} \rightharpoonup u \text{ in } L_2(Q_T) , \quad \overline{\theta}^{(n)} \to \beta(x,u) \text{ in } L_2(I,V) .$$

Remark 3.11. The same convergence results can be obtained when we use the full discretization scheme (also in space) using projection of elliptic problems (2.4)–(2.5) to finite dimensional finite elements spaces $V_\lambda \subset V$ with $V_\lambda \to V(\lambda \to 0)$ in canonical sense.

4 Discussion on numerical experiments

In this section we present numerical experiments demonstrating features of the models (1.1)–(1.3). We compare the results with the multiscale analysis based on the classical anisotropic diffusion equations ([7, 29]).

For computations, we use Approximation schemes 2.1, 2.2 together with the several iterations from Remarks 2.6, 2.7. For the full (scale and space) discretization of the equations one can use either the finite element method ([4, 5]) or the finite volume technique ([25, 28]). The numerical experiments described in this section have been computed using the finite volume spatial discretization of the linear elliptic equations (2.6.1),(2.7.1). The spatial grid is given naturally by the pixel structure of the image. The spatial discretization step for the finite volume method is given as $1/r_1$ with r_1 number of pixels in vertical direction. The Gaussian kernel has been used in the convolution term. Because the discrete image is given by constant values on small squares (pixels), the convolution is reduced to a weighted mean value with weights given by the Gauss function. Since for σ small the weights for pixels with bigger distance are machine zeroes, the averaging is realized only in some bounded neghbourhood. In all presented experiments we use σ such that 7×7 pixels influence the value in the central pixel. As the Perona-Malik function we use $g(s)=1/(1+s^2)$.

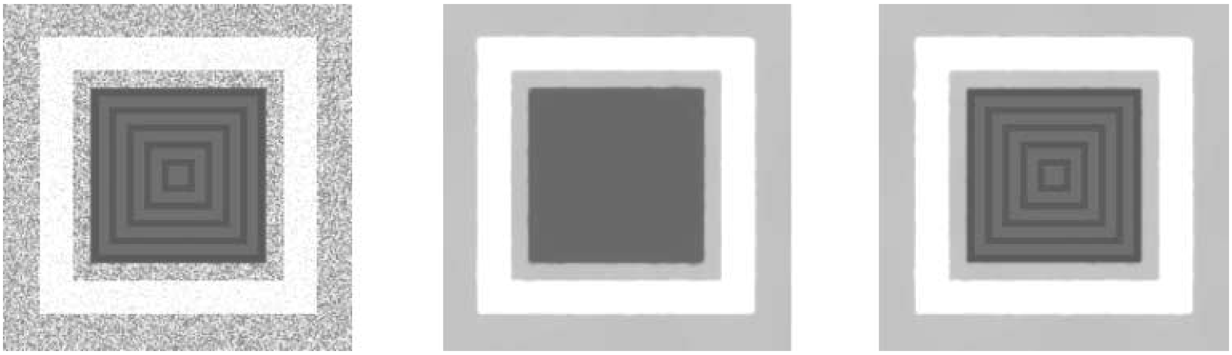

Fig. 1. Restoration of the noisy image (*left*) by the anistropic diffusion (*middle*) and by the anisotropic diffusion coupled with the slow diffusion effect (*right*)

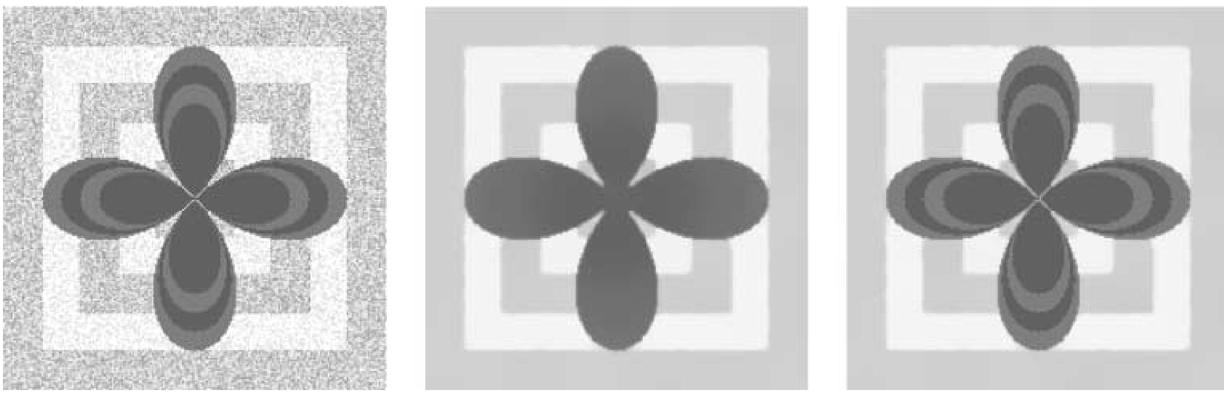

Fig. 2. Restoration of the noisy image (*left*) by the anistropic diffusion (*middle*) and by the anisotropic diffusion coupled with the slow diffusion effect (*right*)

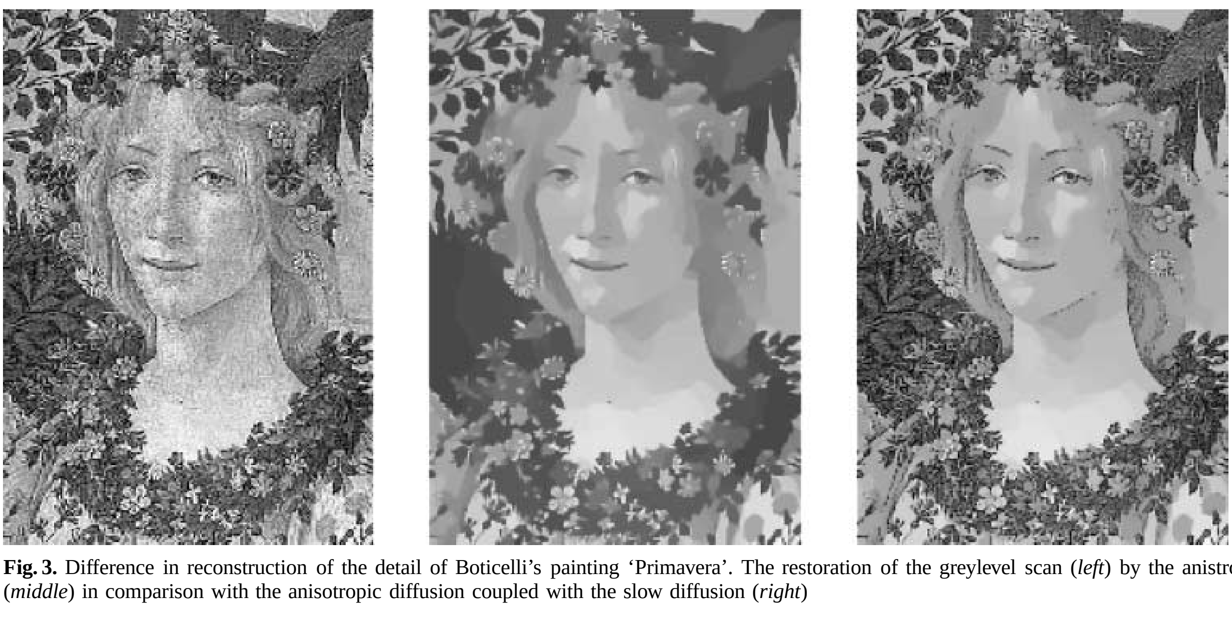

Fig. 3. Difference in reconstruction of the detail of Boticelli's painting 'Primavera'. The restoration of the greylevel scan (*left*) by the anistropic diffusion (*middle*) in comparison with the anisotropic diffusion coupled with the slow diffusion (*right*)

The first, second and fourth processed images consist of 200×200 pixels, the third and fifth ones have the size 570×350 pixels. In Figs. 1–4 we plot the noisy originals (on the left), the results of Catté, Lions, Morel and Coll anisotropic diffusion (in the middle) and the result of application of the slow and fast diffusion effects given by the models (1.1)–(1.3) (on the right). In the last Fig. 5 we present the result of processing of the color image by the anisotropic diffusion coupled with the slow diffusion effect.

Modelling the slow diffusion effect we consider the case **IV**. In addition to CLMC-parameters the function β which is constant for some range of greylevels and linear in complement is used. In presented experiments we consider function $\beta(x, s) = 0$ for $s <= a$, $\beta(x, s) = s - a$ for $s > a$ with some constant a between 0 and 1 (before computations, the image intensity is transformed from integers between 0 and 255 into the real interval $[0, 1]$). In Fig. 1 we present the difference in processing of the initial noisy image (left) by the anisotropic diffusion (middle) and by the anisotropic diffusion coupled with the slow diffusion effect (right) after ten discrete scale steps with step $\tau = 0.001$ in both cases. In case of the slow diffusion, the additional parameters of the method are $a = 0.5$ (in the definition of β function), $K = 10^6$, $d = 0.9$, $\alpha = 0.99$. The choice of β stops the diffusion where we want to keep some fine details in the image (otherwise destroyed by the usual anisotropic diffusion). The same computational parameters have been used in the experiment documented in Fig. 2, we just start

Fig. 4. Processing of the image (*left*) by the anistropic diffusion (*middle*) and by the anisotropic diffusion coupled with the fast diffusion effect (*right*)

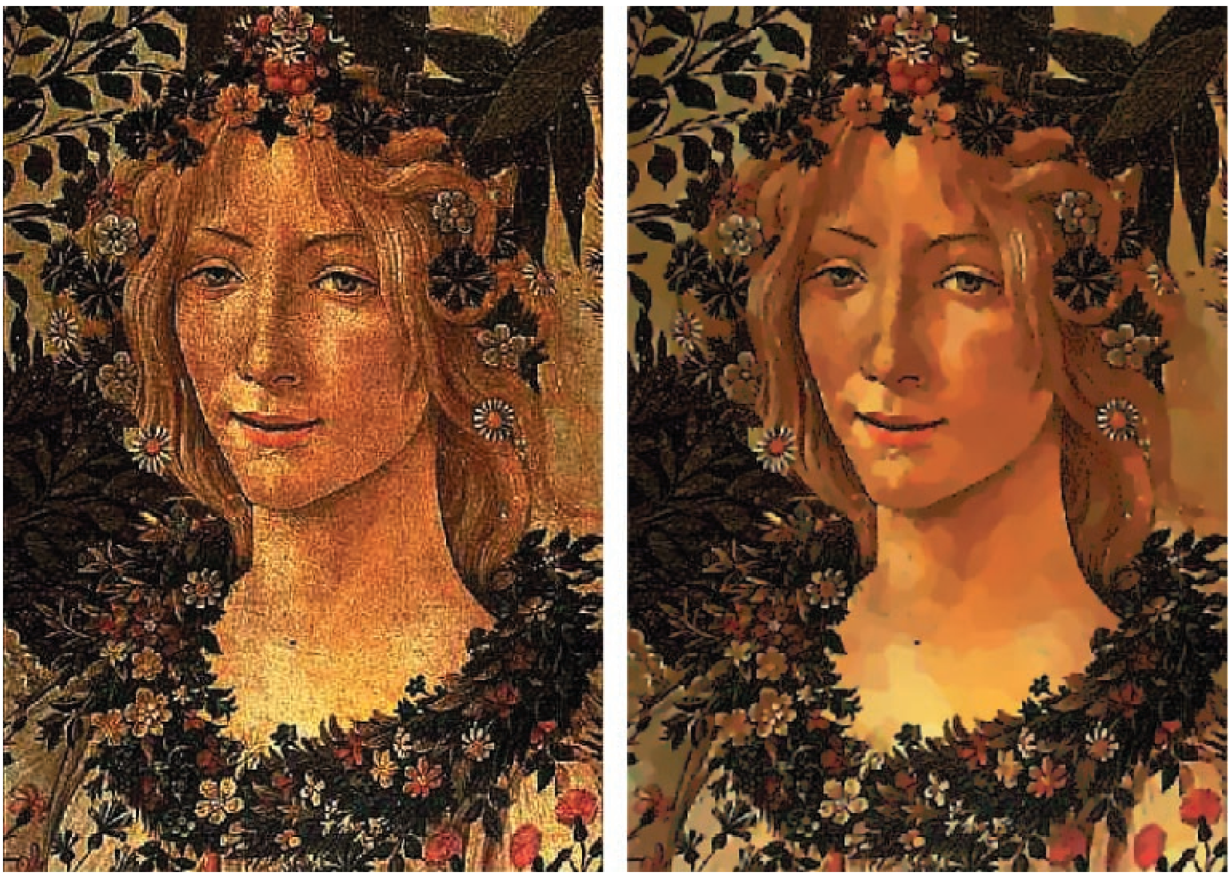

Fig. 5. Reconstruction of the color detail of Boticelli's painting 'Primavera' (*left*) by the anisotropic diffusion coupled with slow diffusion effect (*right*)

from different initial condition. In Fig. 3 we present reconstruction of the greylevel scan of the detail of Botticelli's painting Primavera (left image) by the anisotropic diffusion (middle image) and by the anisotropic diffusion accompanied with the slow diffusion (image on the right). In both cases we plot the results after ten discrete scale steps with step $\tau = 0.001$. In the case of slow diffusion effect we use parameters $a = 0.39$, $K = 10^6$, $d = 0.9$, $\alpha = 0.99$. Using such choice of β, the face is selectively smoothed and the details around are conserved.

In spite of this, if the smoothing of the large structural noise is desirable, the fast diffusion effect can be used. In the experiment presented in Fig. 4, the function $b(x, s) = 0$ for $s <= 0.5$, $b(x, s) = s - 0.5$ for $s > 0.5$, i.e. we consider the case **II**. The scaling versions of the initial image (left) given by the anisotropic diffusion (middle) and coupled with fast diffusion smoothing (right) are plotted at scale 10τ, $\tau = 0.001$. Further parameters were $K = 10^6$, $d = 0.5$, $\alpha = 0.99$.

In Fig. 5 we present application of the anisotropic diffusion coupled with the slow diffusion effect to processing of the RGB color image. We again consider Flora's face detail as the initial condition (left part of Fig. 5). Before processing we divide the color image into red, green and blue chanels. The model (1.1)–(1.3) in the case **IV** is applied to each chanel independently using different choices of the parameters. Then the results of chanel processing are put together in order to get multiscale version of the color original. The result presented in the right part of Fig. 5 has been computed using $K = 10^6$, $d = 0.9$, $\alpha = 0.99$, $\tau = 0.001$ and with different β functions and number of scale steps in the chanels. In the red chanel we use $a = 0.5$ and 5 scale steps, in the green chanel $a = 0.3$ and 7 scale steps and in the blue chanel $a = 0.15$ and 10 scale steps. Let us note that one can consider also a kind of synchronization of chanels processing which will lead to a generalization of (1.1)–(1.3) to degenerate parabolic systems which can be interesting subject for further study.

Acknowledgements. This work was supported by the grant VEGA – 1/7132/20 and by the grant GACR-201/000557. The authors wish also to thank to Professor Willi Jäger for invitation to Interdisciplinary Center for Scientific Computing (IWR), University of Heidelberg, where the important part of this work was finished using the computational facilities of the institute and support of the SFB 359.

References

1. Alt, H.W., Luckhaus, S.: Quasilinear elliptic-parabolic differential equations. Math. Zeitschrift 183, 311-341 (1983)
2. Alvarez, L., Guichard, F., Lions, P.L., Morel, J.M.: Axioms and Fundamental Equations of Image Processing. Arch. Rat. Mech. Anal. 123, 200-257 (1993)
3. Alvarez, L., Morel, J.M.: Formalization and computational aspects of image analysis. Acta Numerica. 1-59 (1994)
4. Bänsch, E., Mikula, K.: A coarsening finite element strategy in image selective smoothing. Computing and Visualization in Science 1, 53-61 (1997)
5. Bänsch, E., Mikula, E.K.: Adaptivity in 3D image processing. Preprint 99-14, Zentrum für Technomathematik, Universität Bremen 1999
6. Berger, A.E., Brezis, H., Rogers, J.C.W.: A numerical method for solving the problem $u_t - \Delta f(u) = 0$. R.A.I.R.O. Anal. Numer. 13, 297-312 (1979)
7. Catté, F. Lions, P.L., Morel, J.M., Coll, T.: Image selective smoothing and edge detection by nonlinear diffusion. SIAM J. Numer. Anal. 29, 182-193 (1992)
8. Gajewski, H., Gröger, K., Zacharias, K.: Nichtlineare Operatorgleichnungen und Operatordifferentialgleichungen. Berlin: Academia-Verlag 1974
9. Handlovičová, A.: Solution of Stefan problem by fully discrete linear schemes. Acta Math. Univ. Comenianae LXVII 2, 351-372 (1998)
10. Jäger, W., Kačur, J.: Solution of porous medium type systems by linear approximation schemes. Num. Math. 60, 407-427 (1991)
11. Jäger, W., Kačur, J.: Approximation of degenerate elliptic-parabolic problems by nondegenerate elliptic and parabolic problems. Preprint, University of Heidelberg 1991
12. Jäger, W., Kačur, J.: Solution of doubly nonlinear and degenerate parabolic problems by relaxation schemes. Mathematical Modelling and Numerical Analysis 29, 605-627 (1995)
13. Kačur, J.: Solution of some free boundary problems by relaxation schemes. SIAM J. Numer. Anal. 36, No. 1, 290-316 (1999)
14. Kačur, J.: Solution to strongly nonlinear parabolic problems by a linear approximation scheme. IMA J. Numer. Anal. 19, 119-145 (1999)
15. Kačur, J., Handlovičová, A., Kačurová, M.: Solution of nonlinear diffusion problems by linear approximation schemes. SIAM J. Num. Anal. 30, 1703-1722 (1993)
16. Kačur, J., Mikula, K.: Solution of nonlinear diffusion appearing in image smoothing and edge detection. Applied Numerical Mathematics 17, 47-59 (1995)
17. Kačur, J., Mikula, K.: Slow and fast diffusion effects in image processing – approximation schemes and numerical experiments. Preprint 96-26 IWR University of Heidelberg 1996
18. Kačur, J., Mikula, K.: Slowed anisotropic diffusion. Scale Space Theory in Computer Vision (ed. by B.M.t.H. Romeny et al.) Lecture Notes in Computer Science 1252, 357-360 (Springer 1997)
19. Krasnoselskij, M., Rutickij, J.: Convex functions and Orlicz Spaces. Moscow: GITTL 1958
20. Kufner, A., John, O., Fučik, S.: Function Spaces. Prague: Academia 1977
21. Lions, P.L.: Axiomatic derivation of image processing models. Mathematical Models Methods in Applied Sciences 4, 467-475 (1994)
22. Magenes, E., Nochetto, R.H., Verdi, C.: Energy error estimates for a linear scheme to approximate nonlinear parabolic problems. Math. Mod. Num. Anal. 21, 655-678 (1987)
23. Mikula, K.: Solution of nonlinear curvature driven evolution of plane convex curves. Applied Numerical Mathematics 23, 347-360 (1997)
24. Mikula, K., Kačur, J.: Evolution of convex plane curves describing anisotropic motions of phase interfaces. SIAM J. Sci. Comput. 17, 1302-1327 (1996)
25. Mikula, K., Ramarosy, N.: Semi-implicit finite volume scheme for solving nonlinear diffusion equations in image processing. to appear in Num. Math.
26. Nečas, J.: Les methodes directes en theorie des equations elliptiques. Prague: Academia 1967
27. Nochetto, R.H., Verdi, C.: Approximation of degenerate parabolic problems using numerical integration. SIAM J. Numer. Anal. 25, 784-814 (1988)
28. Patankar, S.: Numerical heat transfer and fluid flow. New York: Hemisphere Publ. Corp. 1980
29. Perona, P., Malik, J.: Scale space and edge detection using anisotropic diffusion. in Proc. IEEE Computer Society Workshop on Computer Vision 1987
30. Romeny, B.M.t.H. (ed.): Geometry driven diffusion in computer vision. Dodrecht: Kluwer Academic Publishers 1994
31. Slodička, M.: Solution of nonlinear parabolic problems by linearization. in Proc. ISNA'92, Prague 1994